韓國海洋工學會誌 第12卷 第1號, pp.99~106, 1998. 2

◉ 論 文

Open Boundary Modeling for Fully Nonlinear Wave Simulation in a 3-D Numerical Wave Tank

Sung-Youn Boo*

(97년 8월 25일 접수)

3-D 수치 파수조에서 비선형파 시뮬레이션을 위한 방사경계조건의 모델링

부 성 윤*

Key Words : numerical wave tank(파수조), open boundary condition(방사경계조건), boundary element method(경계요소법), nonlinear waves(비선형파)

초 록

3차원 파수조에서 완전 비선형파를 시뮬레이션하기 위하여 우선 랜킨 소스를 기저로한 적분방적식을 고차경계요소법을 이용하여 이산화하였다. 그리고 방사경계조건은 파흡수 비치와 포텐셜 스트레칭 기법을 이용하여 모델링하였으며, 비선형 자유표면파 경계조건식은 고차 예측 및 보정 기법을 이용하여 시간 적분하였다. 파흡수 비치는 파의 진행방향 특성에 따라 수조내에 다양하게 배치할 수 있으며, 비치에서 흡수가 덜된 파는 수조의 길이 방향 끝단에서 포텐셜 스트레칭 기법에 의하여 반사없이 진행하도록 하였다. 수치실험 결과 일-에너지 보존 법칙과 모멘텀-임펄스 보존 법칙이 만족됨으로써 본 수치기법의 효용성이 검증되었다.

1. INTRODUCTION

One of the crucial step for the completion of the nonlinear wave simulation in the numerical wave tank is treatment of open boundary, where non-reflection of the wave is required. The open boundaries enclosing the fluid domain are artificial, and essentially arbitrary. However, the waves propagating to the boundary should be fully transmitted or absorbed. Several modeling schemes for the open boundary condition have been developed. Longuet-Higgens&Cokelet[1] and Xu[2] well applied a periodic condition to the overturning wave simulation. Beer&Watson[3] utilized the infinite element in which the open boundary is mapped to the infinite distance. Orlanski condition[4] has widely been used as a transmitting condition of waves[5),6)]. Arai[7] used the velocity reduction scheme instead of absorbing beach before applying the Orlanski

* 종신회원, 해군사관학교 조선공학과

condition. An absorbing beach scheme was initiated by Cointe[8]. Since then, several different versions of the scheme[9),10),11)] have been reported. Matching scheme of inner solution to outer solution was applied by Dommermuth&Yue[12)].

For the present research, we utilized the combined scheme of absorbing beach and potential stretching. The absorbing beach was firstly distributed near the open boundary. Since the absorbing rate varies according to beach length, it requires an additional scheme to transmit the partially absorbed wave. A potential stretching, therefore, was implemented on the truncation boundary.

Rankine source-based integral equation was discretized by employing a quadratic order boundary element method. The free surface conditions were integrated using the 4th-order predictor-corrector method within the time marching scheme and the location of the free surface was updated every time level.

The Stokes second-order wave was used as an input wave. The wave was gradually fed through the inflow boundary using a wave modulation scheme to reduce an initial transient disturbance. The accuracy of the present numerical scheme was tested using the conservation of energy-workdone as well as momentum-impulse.

2. MATHEMATICAL FORMULATION

The origin of a Cartesian coordinate system is in the plane of the undisturbed free surface with the x-axis positive in the direction of wave propagation and positive x-axis in the opposite direction of the gravity as shown in Fig. 1. It is assumed that the fluid is ideal, incompressible, and its motion is irrotational. The free surface tensions are also ignored and water depth is finite.

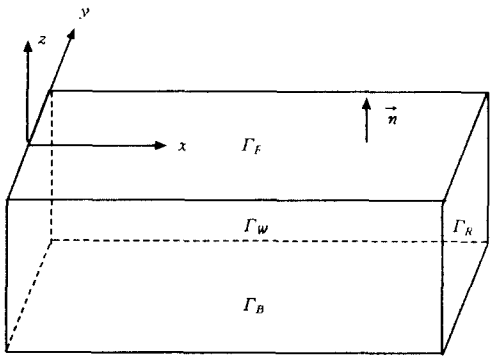

Fig. 1 Coordinate systems and boundary Surfaces

The fluid motion can be described by the total velocity potential of $\phi(\vec{x}, t)$, where $\vec{x}$ is the coordinates (x, y, z) and t the time. The potential $\phi(\vec{x}, t)$ satisfies the Laplace equation

$$\nabla^2\phi(\vec{x}, t) = 0 \tag{1}$$

in the space occupied by the fluid. The kinematic and dynamic free surface conditions on Γ_F are

$$\frac{\partial\zeta}{\partial t} + \frac{\partial\phi}{\partial x}\frac{\partial\zeta}{\partial x} + \frac{\partial\phi}{\partial y}\frac{\partial\zeta}{\partial y} - \frac{\partial\phi}{\partial z} = 0 \tag{2}$$

$$\frac{\partial\phi}{\partial t} + \frac{1}{2}\nabla\phi\cdot\nabla\phi + g\zeta = 0 \tag{3}$$

On flat bottom boundary Γ_B, the following nonpenetrating condition is used.

$$\frac{\partial\phi}{\partial n} = 0 \tag{4}$$

The unit normal vector is denoted by $n = (n_x, n_y, n_z)$ and it is pointing out of the fluid domain. Open boundary condition is imposed on the side boundary Γ_W, upstream boundary and downstream boundary Γ_R.

Since the proposed problem is solved in the time domain, the initial condition must also be satisfied. The condition is

$$\phi(\vec{x}, t) = 0, \quad t \le 0 \quad \text{in the fluid domain} \tag{5}$$

$\eta(\vec{x}, t)=0, \quad t\leq 0$ in the fluid domain

3. FORMULATION OF INTEGRAL EQUATION

The direct boundary integral equation for the velocity potential $\phi(\vec{x}, t)$ is derived using Green's theorem. The resulting equation is

$$\hat{C} + \int_{\Gamma_{S+W}} \phi \frac{\partial G}{\partial n} - \int_{\Gamma_{F+R}} \phi \frac{\partial G}{\partial n} = \int_{\Gamma_{S+W}} G \frac{\partial \phi}{\partial n} - \int_{\Gamma_{F+R}} \phi \frac{\partial G}{\partial n} \tag{6}$$

The solid angle $\hat{C}$ is 0 or 4π when the field point is outside the boundary or in the fluid domain. When the field point is located on the nonplanar boundary, the solid angle is computed using special manner. Two symmetry planes are utilized to model the half fluid domain and exclude the bottom boundary. The Green's function is

$$G=\frac{1}{R_1}+\frac{1}{R_2}+\frac{1}{R_3}+\frac{1}{R_4} \tag{7}$$

The distances between two points are given as:

$$\begin{aligned} R_1 &= \sqrt{(x-x_i)^2+(y-y_i)^2+(z-z_i)^2} \\ R_2 &= \sqrt{(x-x_i)^2+(y+y_i)^2+(z-z_i)^2} \\ R_3 &= \sqrt{(x-x_i)^2+(y+y_i)^2+(z+z_i+2d)^2} \\ R_4 &= \sqrt{(x-x_i)^2+(y-y_i)^2+(z-z_i+2d)^2} \end{aligned} \tag{8}$$

where a is the water depth. The (x, y, z) and (x_i, y_i, z_i) are the field and source point, respectively.

The entire curved boundaries can be approximated by numbers of higher order elements. Within the element, the physical variables are interpolated by higher order polynomials. The resulting approximations are written as:

$$\begin{aligned} \phi &= \sum_j N_j \phi_j \\ \frac{\partial \phi}{\partial n} &= \sum_j N_j \left(\frac{\partial \phi}{\partial n}\right)_j \end{aligned} \tag{9}$$

where N_j is the shape function at the j-th node. The ϕ_j and $(\frac{\partial \phi}{\partial n})_j$ are the velocity potential and normal velocity at the j-th node. We used both nine-node continuous and discontinuous quadrilaterals shown in Fig. 2. The shape functions for those quadrilaterals are well explained in Boo[13].

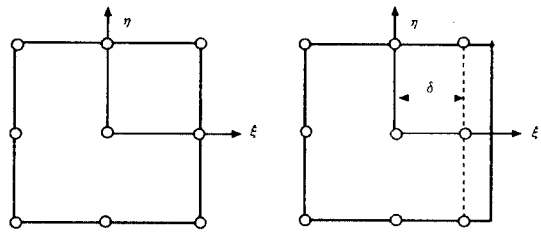

(a) Continuous element (b) Discontinuous element

Fig. 2 Continuous and discontinuous quadrilaterals of quadratic order

By substituting equation (9) into equation (6), the integral equation is represented in the discrete form as:

$$\sum_{k=0}^{NN} \delta_{ik} \hat{C}_i \phi_k + \sum_{k=1}^{NN} \hat{H}_{ik}^{S+W} \phi_k + \sum_{k=N_{S+W}+1}^{NN} \hat{G}_{ik}^{F+R} \left(\frac{\partial \phi}{\partial n}\right)_k$$
$$\sum_{k=1}^{N_{S+W}} \hat{G}_{ik}^{S+W} \left(\frac{\partial \phi}{\partial n}\right)_k + \sum_{k=N_{S+W}+1}^{NN} \hat{H}_{ik}^{F+R} \phi_k \tag{10}$$

where $i=1, 2, \cdots, NN$, NN= total number of nodes, N_S= number of nodes on Γ_S, N_H = number of nodes on Γ_H and

$$\begin{aligned} \hat{H}_{ik}^{S+W} &= \sum_e \sum_j \delta_{kr} \int_{\Gamma_{S+W}} \frac{\partial G}{\partial n} N_j |J| \, d\xi d\eta \\ \hat{H}_{ik}^{F+R} &= \sum_e \sum_j \delta_{kr} \int_{\Gamma_{F+R}} \frac{\partial G}{\partial n} N_j |J| \, d\xi d\eta \\ \hat{G}_{ik}^{S+W} &= \sum_e \sum_j \delta_{kr} \int_{\Gamma_{S+W}} G \, N_j |J| \, d\xi d\eta \\ \hat{G}_{ik}^{F+R} &= \sum_e \sum_j \delta_{kr} \int_{\Gamma_{F+R}} G \, N_j |J| \, d\xi d\eta \end{aligned} \tag{11}$$

δ_{ik}, δ_{kr}= Kronecker delta function

where r is the node number at the j-th node on the e-th element, e the element number and $|J|$ the Jacobian.

Since the discretized integral equation is variant in time, all the boundary surfaces are regridded at each time step. The influence coefficients are also recomputed using the updated grids.

4. OPEN BOUNDARY MODELING

The open boundary is modeled by the following manners. Firstly, the absorbing beach is placed in the longitudinal as well as transverse direction of the tank in order to partially absorb the waves as shown in Fig. 3. The dynamic free surface condition on the beaches can be written as:

$$\frac{\partial \phi}{\partial t} + \frac{1}{2} \nabla \phi \cdot \nabla \phi + g\zeta + \mu\phi = 0 \tag{12}$$

where the tuning factor μ is determined in the following equations,

$$\begin{aligned} \mu = \ & \mu_x && : \ \bar{x} > x_b,\ \bar{y} < y_b \\ & \mu_y && : \ \bar{x} < x_b,\ \bar{y} < y_b \\ & \mu_x + \mu_y && : \ \bar{x} \geq x_b,\ \bar{y} \geq y_b \\ & 0 && : \ \text{otherwise} \end{aligned} \tag{13}$$

where

$$\begin{aligned} \mu_x &= 2\left(\frac{\bar{x} - x_b}{L_x}\right)^2 \\ \mu_x &= 2\left(\frac{\bar{y} - y_b}{L_y}\right)^2 \times \tanh\frac{3\bar{x}}{\lambda} \end{aligned} \tag{14}$$

Here x_b is the distance from the inflow boundary to the longitudinal beach-front while y_b is the distance from the centerline of the tank to the transverse beach-front. The coordinates $\bar{x}$ and $\bar{y}$ are measured from the inflow boundary and the centerline of the tank, respectively. The term of $\tanh\frac{3\bar{x}}{\lambda}$ in μ_y is introduced to allow gradual increment of damping in the longitudinal direction and λ is the wave length.

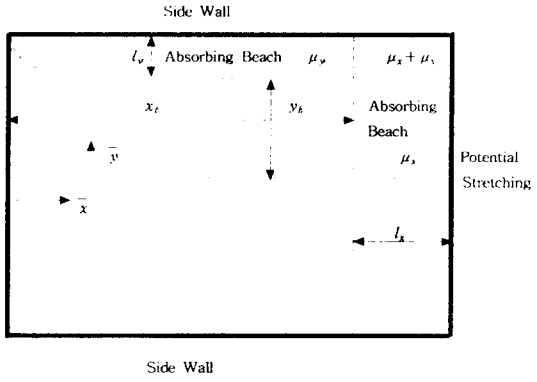

Fig. 3 Modeling of open boundary using absorbing beach and potential stretching for open boundary condition

Secondly, a stretching method is applied to the outflow boundary (Fig. 4). The resulting equations of the stretching for the velocity potential and velocity are

$$\phi(\vec{x}, t) = \phi_o(\vec{x}, t)\frac{\cosh k(z_e + d)}{\sinh kd} \tag{15}$$

$$\frac{\partial \phi(\vec{x}, t)}{\partial n} = \frac{\partial \phi_o(\vec{x}, t)}{\partial n}\frac{\cosh k(z_e + d)}{\sinh kd} \tag{16}$$

where $\phi_o(\vec{x}, t)$ is the velocity potential on the instantaneous free surface at the upper edge of the open boundary and k the wave number. The mapped z-coordinate z_e is defined as

$$z_e = \frac{(z + d) \times d}{\zeta_o + d} - d \tag{17}$$

where d is the water depth and ζ_o the location

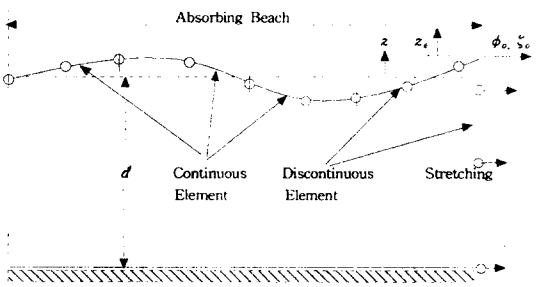

Fig. 4 Potential stretching on the open boundary

of the instantaneous free surface at the upper edge of the open boundary.

Lastly, in treating the boundary condition on the inflow boundary, stretching scheme which is analogous to one on the outflow boundary is employed. The mapped coordinate on the boundary is

$$z_e = \frac{(z+d)}{\zeta_o + d} \times (d + \zeta_i) - d \tag{18}$$

where ζ_i is ζ of the incident wave. The velocity potentials and velocities on the boundary are computed using the coordinates and utilized for the input wave generation.

5. CHECKS OF ACCURACY

A global check of the time stepping accuracy is provided by the volume error relative to the initial volume[14]. The total volume (V_x, V_y, V_z) of the fluid in the three directions is computed using

$$(V_x, V_y, V_z) = \sum_e \int_e (xn_x, yn_y, zn_z) d\Gamma \tag{19}$$

The total energy E_t and workdone W should balance in the fluid where E_t is the sum of the potential energy E_p and the kinetic energy E_k

$$\begin{aligned} E_t &= E_p + E_k \\ &= \frac{1}{2} \sum_e \int_e z^2 n_z d\Gamma + \sum_e \int_e \phi \frac{\partial \phi}{\partial n} d\Gamma \end{aligned} \tag{20}$$

$$W = \sum_e \int_0^t \int_e p \frac{\partial \phi}{\partial n} d\Gamma \, dt \tag{21}$$

The conservation of the total momentum (M_x, M_y, M_z) and impulse (I_x, I_y, I_z) in the three directions is computed using

$$(M_x, M_y, M_z) = \sum_e \int_e (\phi n_x, \phi n_y, \phi n_z) d\Gamma \tag{22}$$

$$(I_x, I_y, I_z) = \sum_e \int_0^t \int_e (p n_x, p n_y, p n_z) d\Gamma \, dt \tag{23}$$

6. NUMERICAL RESULTS

The continuous quadratic element was used to discretize the enclosed boundary except the intersection region near the downtank boundary, where the partially discontinuous element with parameter $\delta = \frac{2}{3}$ was distributed.

The fourth-order Adams-Bashforth-Moulton method was applied to integrate the free surface conditions. The second-order Stokes waves were fed through the inflow boundary. The waves at the inflow boundary increased gradually using a modulation function which satisfies the initial calm water condition. The modulation time was chosen as one wave period. A numerical instability was avoided by employing the appropriate time increment of $\Delta t \le \frac{T}{60}$, where T is the period of the incident wave. The wave elevation, velocity potential, normal derivative of potential, and velocities were filtered every two time step using five neighboring points in the longitudinal as well as transverse direction of the tank. The elevation of the simulated wave was normalized by the amplitude of the incident wave. The principal dimensions of the wave tank are length × width × depth = $12R \times 6R \times 1.16R$ where R denotes the unit length. The beach length is half of the wave length and the beach is placed at the 3/4 tank length from the inflow boundary. The parameters of the incident waves were $A/d = 0.1$, $d/R = 1.16$ and $kR = 1.3$

The simulation was performed for the two different cases. Firstly, we simulated the fully nonlinear wave in a rectangular wave tank. Wave elevations were measured at the four different locations. The locations are the inflow boundary B, tank center D, beach-front E and beach-end F as shown in Fig. 5. The absorbing rate of the wave on the beach is found to be about 50 percents for the beach length of 0.5λ.

It has been reported that beach length chosen affects absorption. This will be investigated further in the following test.

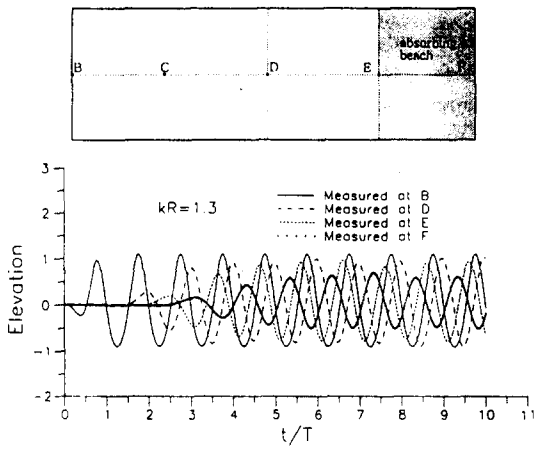

Fig. 5 Wave elevations time histories measured at the various locations of the tank

The percent error of the fluid volume relative to the initial one is compared in Fig. 6. The error oscillates in the time but within 2 percents. The balance of the total energy and workdone by the fluid is investigated in the Fig. 7. The values increase gradually until the waves are fully developed. It is shown that both the energy and workdone are well conserved. Further validation is made using the momentum-impulse conservation in Fig. 8 and Fig. 9. The values in the x and z directions are shown to be well balanced.

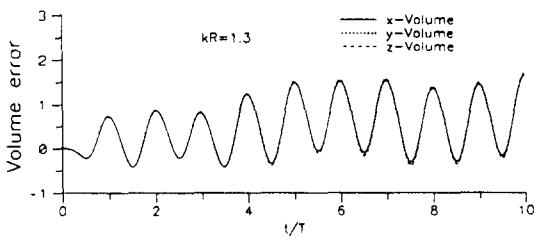

Fig. 6 Volume error(%) in the x, y and z-directions

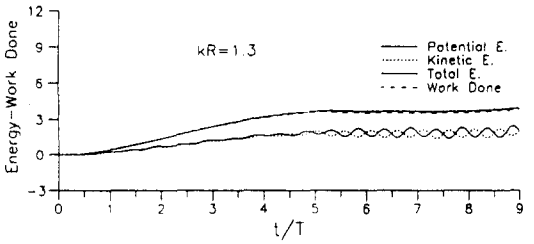

Fig. 7 Balance check of the energy and work-done

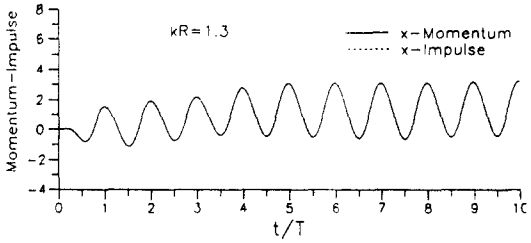

Fig. 8 Balance check of the momentum and impulse in the x-direction

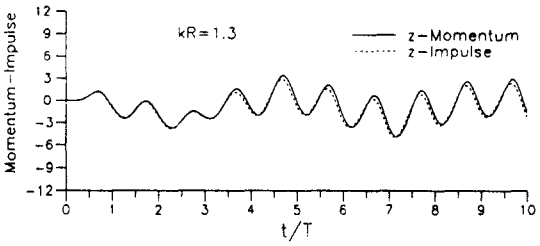

Fig. 9 Balance check of the momentum and impulse in the z-direction

Secondly, the nonlinear wave was simulated in the non-rectangular shaped tank in order to investigate three dimensional effect as well as absorbing rate of wave. The tank length varies $12R$ to $15.6R$. The distances from the beach-front to the four beach-end points of D, E, F and G are about 0.5λ, 0.73λ, 1.0λ and 1.25λ, respectively. The time histories of the wave elevation at the four locations are shown in Fig. 10. It can be seen that the absorption of the waves varies with the beach length as it is

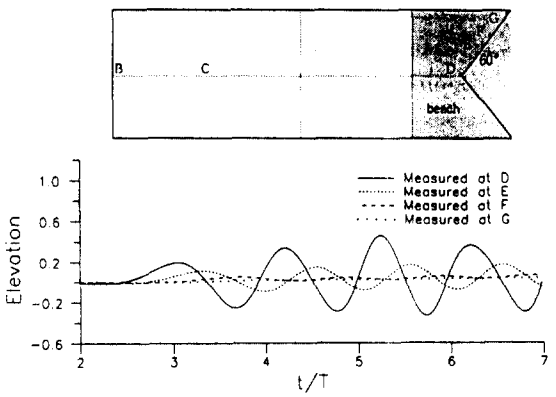

Fig. 10 Artificial damping effect on the beach

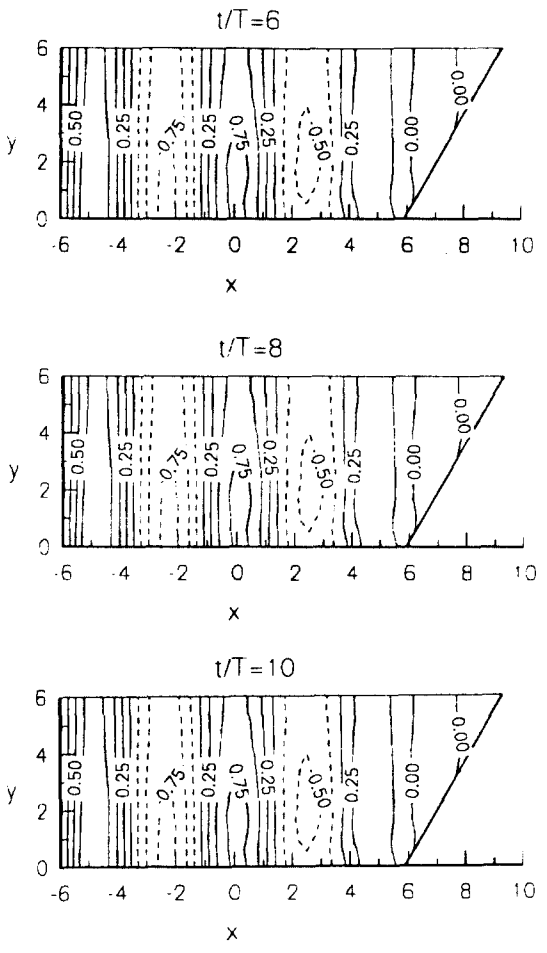

Fig. 11 Wave contour at the various time instants

expected from the tuning factor given in equation (13). The waves at F and G where the beach lengths are bigger than one wave-length, were almost dampened. It can be stated that at least one wave length beach should be furnished for the complete absorption in the present modeling. The modeling was also examined by comparing the wave contours for the different duration of simulation shown in Fig. 11. Reflections due to the present scheme for the open boundary modeling are not found.

7. SUMMARY AND CONCLUSIONS

The overall numerical scheme for the simulation of either nonlinear or even linear waves highly depends on the method of the open boundary modeling. The aim of the present work is, therefore, to develope a numerical scheme in treating the open boundary condition for the fully nonlinear wave simulation in the time domain. The modeling scheme was established in the 3D numerical wave tank which has inflow, outflow, side and bottom boundaries. A combined condition of a numerical absorbing beach with a potential stretching was introduced for the present open boundary modeling. The numerical beach scheme has widely been applied. However, since the absorbing rate of the wave fields varies with the beach length, it may not be easy to set an appropriate beach in the tank in order to take into account from a short wave to long wave. Because of that reason, we introduced an additional device called potential stretching to the truncation boundary. The function of the stretching is to fully transmit waves which may not be absorbed on the beach.

A quadratic order boundary element method was utilized to approximate the integral equation based on Rankine source. The free surface conditions were integrated every time step using

the 4th-order predictor-corrector method. The fully nonlinear wave was simulated by satisfying all the prescribed boundary conditions. The Stokes second-order wave was used as an input wave which was modulated for initial one wave period. It was found that the beach length should be bigger than one wave length for the complete absorption. The performances of the present numerical scheme were investigated by checking the conservation of energy and workdone as well as balance of momentum and impulse. They are proven to be well conserved during the simulations.

ACKNOWLEDGMENT

This research is supported in part by Korea Science and Engineering Foundation under contract 941-1000-031-2.

REFERENCES

1) Longuet-Higgins,M.S., & Cokelet,E.D., "The Deformation of Steep Surface Waves on Water-I. A Numerical Method of Computation", Proc. Roy. Soc. Lond, A. 350, 1-26, 1976.

2) Xu,H., "Numerical Study of Fully Nonlinear Water Waves in Three Dimensions", Sc.D Dissertation, Dept. of Ocean Engineering, Massachusetts Institute of Technology, Cambridge, U.S.A., 1992.

3) Beer,G. & Watson,J.O., "Infinite Boundary Element", *International Journal for Numerical Methods in Engineering*, Vol 128, 1233-1247, 1989.

4) Orlanski,J.E., "A Simple Boundary Condition for Unbounded Hyperbolic Flows", *Journal of Computational Physics*, Vol. 21, 251-269, 1976.

5) Boo,S.Y., Kim,C.H. & Kim,M.H., "A Numerical Wave Tank For Nonlinear Irregular Waves by 3-D Higher Order Boundary Element Method", *International Journal of Offshore and Polar Engineering*, Vol. 4, No. 4, 1994.

6) Isaacson,M. & Cheung,K.F., "Time-Domain Second-Order Wave Diffraction in Three Dimensions", *Journal of Waterway, Port, Coastal & Ocean Engineering*, ASCE, Vol. 118, No. 5, pp. 495-516, 1992.

7) Arai,M., Paul,U.K., Cheng,L.-Y. & Inoue,Y., "A technique for Open Boundary Treatment in Numerical Wave Tanks", *Journal of the Society of Naval Architects of Japan*, Vol. 173, 45-50, 1993.

8) Cointe,R., "Nonlinear Simulation of Transient Free Surface Flows", *Proc. of the 5th International Conference on Numerical Ship Hydrodynamics*, Hiroshima, Japan, 239-250, 1989.

9) Boo,S.Y. & Kim,C.H., "Fully Nonlinear Diffraction Due to a Vertical Cylinder in a 3-D HOBEM Numerical Wave Tank", *Proc. 6th ISOPE Conference*, Vol. III, pp. 23-30, L.A., U.S.A., 1996.

10) Clement, A., "Coupling of Two Absorbing Boundary Conditions for 2D Time-Domain Simulations of Free Surface Gravity Waves", *J. Computational Phisics*, Vol. 126, pp. 139-151, 1996.

11) Skourup, J., "Active Absorption in a Numerical Wave Tank", *Proc. 6th ISOPE Conference*, Vol. III, pp. 31-38, L.A., U.S.A., 1996.

12) Dommermuth,D.G., & Yue,D.K.P., "Numerical Simulations of Nonlinear Axisymmetric Flows with a Free Surface", *Journal of Fluid Mechanics*, Vol 178, 195-219, 1987.

13) Boo,S.Y., "Application of Higher Order Boundary Element Method to Steady Ship Wave Problem and Time Domain Simulation of Nonlinear Gravity Waves", Ph.D Thesis, Ocean Engineering Program, Texas A&M University, U.S.A., 1993.

14) Tanizawa, K., "A Nonlinear Simulation Method of 3-D Body Motions in Waves", *JSNAJ*, Vol. 178, pp. 180-191, 1995.